九州大学学術情報リポジトリ
Kyushu University Institutional Repository

Application of particle simulation methods to composite materials: A review

Yashiro, Shigeki
Department of Mechanical Engineering, Shizuoka University

https://hdl.handle.net/2324/4476073

出版情報：Advanced Composite Materials. 26 (1), pp.1-22, 2016-08-25. Taylor and Francis
バージョン：
権利関係：

KYUSHU UNIVERSITY

Advanced Composite Materials, 2017, Vol. 26, No. 1, 1–22
DOI: 10.1080/09243046.2016.1222508

Application of particle simulation methods to composite materials: A review

Shigeki Yashiro [1,*]

[1] Department of Mechanical Engineering, Shizuoka University

3-5-1 Johoku, Naka-ku, Hamamatsu 432-8561, Japan

* Corresponding author: yashiro.shigeki@shizuoka.ac.jp

Abstract

Particle simulation methods represent deformation of an object by motion of particles, and their Lagrangian and discrete nature is suitable for explicit modeling of the microstructure of composite materials. They also facilitate handling of large deformation, separation, contact and coalescence. Mesh-free particle methods will thus be appropriate for a part of issues throughout the lifecycle of composite materials despite their high calculation cost. This study focuses on three particle simulation methods, namely, smoothed particle hydrodynamics, moving particle semi-implicit method, and discrete element method, and reviews approaches for modeling composite materials through these methods. Applicability of each method as well as advantages and drawbacks will be discussed from the viewpoint of engineering of composite materials. This reviewing study suggests capability of particle simulation methods to handle multiphysics and to predict various complex phenomena that necessitate explicit modeling of the material's microstructure consisting of reinforcements (inclusions), matrix, and voids.

Keywords: Composite materials; Microstructure; Impact; Molding; Damage accumulation; Fluid-solid interaction; Smoothed particle hydrodynamics (SPH); Moving particle semi-implicit (MPS) method; Discrete element method (DEM)

1. Introduction

Advanced composite materials have frequently been used in aerospace industry taking advantage of their high specific strength and stiffness as well as good fatigue properties. The favorable characteristics enhance their use in weight saving applications including car industry. Failure and strength of prepreg-based continuous fiber reinforced composites were the major topic till early 2000s. But with increasing use of composite materials, these materials have encountered a wide variety of challenges [1], which include manufacturing and processing, interfaces and interphases, fracture and damage, fatigue, dynamic behavior, damage tolerance, nondestructive evaluation, and recycling. Meanwhile, there are many reinforcing materials and configurations as well as various matrix materials. Experimental evaluations require too many laborious efforts to address these issues, and the analytical approaches are thus required.

The most widely used numerical method is definitely the finite-element method (FEM). However, the preprocess for a complex shape generally requires great efforts and experiences for mesh adjustments and checks. Therefore, the significant improvement of computation powers has not contributed to reduction of the total time consumed from pre-process to post-process. Sophisticated techniques are often needed to solve problems concerning large deformation and moving discontinuity (e.g., crack extension in solids). Existence of the mesh is the fundamental cause of these issues.

Mesh-free methods provide an alternative way to tackle these tough problems. Smoothed particle hydrodynamics [2-4] is one of the major mesh-free methods. Another most popular mesh-free methods are the element-free Galerkin method [5-7], the reproducing kernel particle method [8,9], and the meshless local Petrov-Galerkin method [10-13]. These methods have been applied to analyses of laminated and functionally graded materials [14], and a good review on various mesh-free methods and their implementation is found in literature [15]. These

methods facilitate pre-processing and handling of moving discontinuity thanks to absence of a mesh. The major drawback is extremely high calculation cost compared with FEM. Moreover, strict application of Dirichlet boundary conditions (e.g., fixed displacements in structural analysis) requires special algorithm in the analytical framework.

Some mesh-free Lagrangian methods represent deformation of a continuum by motion of particles. They can easily handle large deformation, separation, contact and coalescence, and this characteristic is useful to predict behavior of composite materials under some particular conditions. This study therefore aims to review particle-based modeling of composite materials found in literature, and focuses on three methods, namely, smoothed particle hydrodynamics (SPH), moving particle semi-implicit (MPS) method, and discrete element method (DEM). Although several decades have passed since these numerical methods were developed, their applications to composite materials are still limited probably because of the high calculation cost. Meanwhile, with expanding use of composite materials, phenomena to be solved have become more complicated in recent years. Particle simulation methods will be appropriate for analyses of a part of challenges throughout the material's lifecycle from fabrication to disposal/recycle, even if severe drawbacks are considered.

2. Smoothed particle hydrodynamics (SPH)

2.1 Fundamental theory – interpolation method

SPH had been developed to predict astrophysical compressible flow [16,17], and has recently been used to analyze incompressible flow [18], viscous flow [19-22], and solid mechanics [23-27]. Detailed formulation is found in literature [2-4,26-28]. SPH is a mesh-free Lagrangian method that uses particles representing a continuum. The fundamental concept of SPH is an interpolation theory that allows a function to be expressed in terms of its value at a set of

disordered points using a kernel function. The kernel function refers to a weighting function of a particle and specifies the contribution of a variable ϕ at position $\mathbf{x}$. The spatial distribution of ϕ is obtained by superposition of the kernel function W.

$$\phi(\mathbf{x}) = \int_D \phi(\mathbf{x}')W(\mathbf{x}-\mathbf{x}',h)\mathrm{d}\mathbf{x}' \approx \sum_{b=1}^{N} \phi_b \frac{m_b}{\rho_b} W(\mathbf{x}-\mathbf{x}_b,h) \tag{1}$$

Here, m and ρ are the mass and density of a particle. D is the solution volume, and the smoothing length h denotes the effective width of the kernel, which is typically the cubic B-spline function. Subscript b denotes the index of a neighboring particle, and N is the number of particles in the effective radius. Using the divergence theorem of Gauss and the fact that W vanishes at infinity, a particle equation for the gradient can be obtained as

$$\langle \nabla \phi(\mathbf{x}) \rangle = \int_D \phi(\mathbf{x}')\nabla W(\mathbf{x}-\mathbf{x}',h)\mathrm{d}\mathbf{x}' = \sum_{b=1}^{N} \phi_b \frac{m_b}{\rho_b} \nabla W(\mathbf{x}-\mathbf{x}_b,h). \tag{2}$$

This equation indicates that the gradient of a variable is calculated by the differential of the kernel function, and therefore, the governing equations of continuum mechanics (i.e., conservation of mass, momentum and energy) are discretized without a mesh. SPH-based structural analyses suffers numerical instability under tensile stresses, and reduction of this "tensile instability" has been investigated [26,27,29-32].

2.2 Applications

Various applications of SPH are found in fluid and solid mechanics in mechanical engineering and the other fields, e.g., dams and tsunami in civil engineering, and lava flow in geo-engineering [4,33].

2.2.1 High- and hyper-velocity impact on composites

High- and hyper-velocity impact of foreign objects on composite materials is a typical

application of SPH, since it can easily handle indentation and following fragmentation. In addition, the high calculation cost is alleviated because of the short-time phenomenon and of the localized deformation requiring a small analytical model.

An elasto-plasticity material model [34] and a visco-plasticity material model [35] for unidirectional composites have been developed and implemented into SPH to address perforation induced by impact loading. Hayhurst et al. [36] developed macro-mechanical material models of woven ceramic fabric and Kevlar/epoxy composite used in a bumper shield system to predict failure phenomena of a multi-shock shield. Hypervelocity impact on a CFRP target and a CFRP/AFRP bonded target plate was analyzed with experimentally identified material properties for the macro-mechanical material model [37].

Chen and Medina [38] modeled a B/Al cross-ply laminate as an inhomogeneous medium, not a homogeneous anisotropic medium, to predict detailed impact damage. Thick boron fibers allowed fiber/matrix explicit modeling. However, SPH has difficulty in defining clear material interfaces because of the interpolation equation (1), and therefore, such modeling approach for composites is hardly found in literature. Shintate and Sekine [39] incorporated a particle generation and particle merger technique in hypervelocity impact simulations on CFRPs. This improved technique prevented numerical fractures, i.e., unrealistic separation of particles not satisfying failure criteria, conserving total energy of the overall system

Although some materials models and advanced numerical algorithms have been developed, the fundamental SPH framework have been used to analyze high-velocity impact on CFRP laminates [40] and alumina/aluminum composites [41], hypervelocity impact on cryogenically cooled aluminum alloys and composites [42], and impact of an explosive-filled fragmenting shell into double-plate bumper structure (steel plate and GFRP) [43].

2.2.2 Coupled FE-SPH hypervelocity impact simulations for composites

All of the target and projectile in the analytical models described in the previous section were discretized by particles. However, in many practical applications, SPH is used only in a part of a model, and the remaining part is analyzed by FEM. Such modeling is attributed mainly to the high calculation cost of SPH. Implementation of SPH into commercial software for dynamic simulations allows partial application of SPH. The coupling algorithm of SPH and FEM is found in literature [44].

Hypervelocity impact on composite targets have been analyzed for satellites and the international space station (ISS) since late 2000s. Projectiles and a part of target plates, which broke down into many fragments, have been modeled by SPH. A series of simulations [36,37,45-49] have been performed concerning hypervelocity impact on the Columbus module of ISS and satellite walls. The macro-mechanical material model [36] had been further improved to take into account nonlinear orthotropic constitutive behavior [45,46]. Shielding response of the first bumper (aluminum alloy) and intermediate composite layers was predicted by SPH, and the back wall was modeled by Lagrangian finite elements [45]. In the case of honeycomb structures [48,49], a part of the front face-sheet was modeled with SPH and was joined to a Lagrangian volume element grid, and shell elements were used for the honeycomb core. Optimization of the Whipple shield system has been investigated by combining the coupled FE-SPH simulation with optimization techniques [50,51].

A similar approach has been employed in the following studies along with more detailed FE modeling for composite materials. Cherniaev and Telichev [52] analyzed hypervelocity impact on a composite overwrapped pressure vessel to investigate the effect of filament winding patterns on vessel damage. SPH particles were used for both aluminum projectile and aluminum shielding plate to represent fragmentation, whereas a Lagrangian FE mesh was utilized for the

front wall of the composite vessels for accurate description of interfacial behavior. Their model was further improved to analyze meso-scale behavior of composite laminates, which included FE-modeling of individual plies and resin-rich interlayers and delamination, but SPH was used only in the projectile to represent its deformation and fragmentation [53].

2.2.3 Bird strike on composite structures

Birds flow in a fluid-like manner over the target structure at a high velocity of interest. Soft-body impact is thus a challenging problem, because the impact force distribution and its variation with time depend on the large deformation of the target and projectile [54]. SPH is appropriate for such a phenomenon.

A good review on bird strike simulations and soft-body bird impactor models [55] pointed out that, after a long period of development, there are still three techniques widely used, i.e., Lagrangian FEM, Eulerian or Arbitrary Lagrangian-Eulerian (ALE) FEM, and SPH. All of them have their own advantages and drawbacks. SPH has numerical robustness against large deformation, thanks to absence of a mesh. However, dense particles are required for a given volume to obtain adequate behavior, and resulting high calculation cost is the major drawback. Lack of sharp boundaries due to Eq. (1) may affect the definition of fluid-structure interaction.

Most of soft-body impact simulations on composite structures used SPH only for projectiles (gelatin substitutes) [56-64], although gelatin could not reproduce sliding of birds [65]. This is because an aircraft structure modeled by SPH particles provokes unrealistically high calculation cost, when considering inhomogeneous microstructure of composite materials. Again, see Ref. [44] for interaction algorithm between SPH and FEM.

2.2.4 Other impact problems

Dynamic interaction between a structure and a fluid (i.e., hydro-elastic phenomena) can be observed in aeronautical, naval and sporting applications. A review on the water entry problems for aeronautical structures is found in literature [66], suggesting SPH as a possible tool to study such problems. FE-SPH coupling approach have been employed for water-entry simulations, and SPH has been applied to water [67-70], similarly to soft-body impacts. Comparison study among other methods like ALE-FEM pointed out the high calculation cost of SPH [67,70].

The other fluid-structure interaction problem is hydrodynamic ram event; the most well-known accident is the Concorde accident in 2000. A high-velocity impact of a steel sphere into a partially water-filled CFRP woven laminate tank was simulated [71]. Lagrangian FEM was used to discretize the surrounding composite structure and the projectile, and the water was modeled by ALE-FEM or SPH. Both water models predicted well the overall process of the phenomenon, but high calculation cost of SPH was an obstacle for a large-scale simulation.

Behavior of a composite sandwich panel against blast wave was also predicted through the same approach, and trinitrotoluene charge and resulting blast wave were discretized by SPH particles [72]. Behavior of gaseous products of detonation was described by the conservation equations and the Jones-Wilkins-Lee equation of state.

2.2.5 Fabrication of composites

Resin flow during composite molding process has been analyzed by SPH. The governing equations to be solved are the mass conservation equation and the Navier-Stokes equation. Comas-Cardona et al. [73] analyzed RTM of composite/foam-core sandwich using coupled FE-SPH method to address the hydro-mechanical coupling. SPH particles and Lagrangian finite elements were used to represent the viscous resin and the elastic foam core. Deformation of the foam core due to resin pressure induced flow different from the initial condition because of

permeability variations and the formation of new channels. Hall et al. [74] applied SPH to mending process in self-healing composites. Resin filling process into an opened crack was capillary flow, and the surface tension was taken into account as an external force.

SPH was also applied to flow of fiber suspension, and short steel fiber reinforced concrete was assumed to be a mixture of a non-Newtonian incompressible fluid and rigid bodies [75]. A rigid fiber was represented by two connected particles positioned at fiber ends. Such explicit fiber modeling enables us to monitor orientation and distribution of fibers throughout the molding process.

A mesoscopic model for fabrication process of ceramic-matrix composites (CMCs) was developed using SPH. Solid-solid reaction was analyzed based on the continuity equation, the energy equation and the species equation, and evolution of the microstructure was predicted with heat flux [76]. Reaction between SiC matrix and filler particles (U_3O_8) was accompanied by continuous variation of composition, porosity and material properties. Lagrangian nature of SPH was suitable for handling filler shrinkage and resulting porosity change. Suitability to tackle multiphysics problems is an advantage of SPH, although the original SPH cannot define clear boundaries or material interfaces.

2.2.6 Advanced modeling in SPH

Chen et al. [77] proposed Lagrangian corrected SPH, which could define clear material interface discontinuities, to investigate debonding process in particulate composites. Explicit interfaces allowed the use of the cohesive zone model that provided a continuous interfacial traction but a displacement jump across interface. The material virtual work equation was written by the framework of SPH, and the resulting weak form equation was solved implicitly to compute the displacement field and its derivation. To obtain SPH expression for the

interfacial displacement constraint conditions, a spring potential function was defined, and a bi-linear traction-separation relation was applied to material interfaces.

Lin et al. [78] proposed shell-based SPH to address reduction of calculation cost. The governing differential equations of thin structures was based on a first-order shear deformation plate theory considering the geometrically nonlinear behavior. SPH strong formulation using the total Lagrangian framework was employed to avoid tensile instability, and the boundary deficiency was alleviated by a corrective smoothed particle method [79,80]. Several benchmark analyses involving large deformations of laminated structures were treated successfully by the shell-based SPH. Moreover, the shell-based SPH was applied to low-velocity impact on composite multilayered plates [81]. A single particle layer could not provide accurate contact pressure through the usual SPH algorithm. Nonlinear contact law of Hertz was then adopted to describe the relationship between the impact force and the indentation, considering the projectile as a rigid sphere. Difficulty in handling contact may become a limitation for solving a general impact problem accompanied by deformation of a projectile.

Yashiro and Okabe [82] proposed the other approach to reduce calculation cost by solving SPH equations in a generalized coordinate system. This method achieved non-uniform initial particle arrangement; more specifically, particles were first allocated with a fine spacing in a direction required, and the particles were rearranged in a generalized coordinate system with a constant spacing in three directions. A soft-body impact simulation was performed by using SPH particles for all of the composite laminate and the gelatin projectile [83]. Figure 1 depicts the simulation results and corresponding high-speed camera images; the predicted deformation state agreed with the observation. This result demonstrated that the new approach could reproduce dynamic behavior of composite materials with a reduced calculation cost, while maintaining the intrinsic advantage of easy handling of large deformation and contact.

2.3 Summary

SPH is a dynamic numerical method for continua, and its major advantage is easy handling of large deformation, contact and separation. In addition, SPH can be applied to various phenomena governed by differential equations because of the simple expression for differential of a field variable. SPH is therefore appropriate for multiphysics simulations. Some commercial dynamic FE codes incorporate SPH into their simulation frameworks, which facilitate a coupled FE-SPH simulation.

The major drawback is the high calculation cost. When using fine particles to represent a microscopic structure of composite materials, the whole target will take unrealistic calculation cost due to the enormous number of particles. Moreover, update of the neighboring particle list, which is a time consuming routine, should be repeated at a short interval. Lack of a clear interface (discontinuity) due to the expression for the spatial distribution will also be a drawback for composite materials having inhomogeneous microstructures. This characteristic causes difficulty in analyzing interfacial behavior, e.g., incorporation of the cohesive zone model.

3. Moving particle semi-implicit (MPS) method

3.1 Differential operator models

MPS method is a new particle-based numerical method for continua, particularly for incompressible viscous flow [84,85], but is applicable to solids [86]. Its formulation is found in literature [84,85,87]. The following differential operator models are the fundamental concept to discretize differential equations.

$$\langle \nabla \phi \rangle_a = \frac{d}{n_0} \sum_{b \neq a} \left[\frac{\phi_b - \phi_a}{|\mathbf{r}_b - \mathbf{r}_a|^2} (\mathbf{r}_b - \mathbf{r}_a) \, w(|\mathbf{r}_b - \mathbf{r}_a|) \right] \tag{3}$$

$$\left\langle \nabla \cdot \mathbf{u} \right\rangle_a = \frac{d}{n_0} \sum_{b \neq a} \left[\frac{(\mathbf{u}_b - \mathbf{u}_a) \cdot (\mathbf{r}_b - \mathbf{r}_a)}{|\mathbf{r}_b - \mathbf{r}_a|^2} w(|\mathbf{r}_b - \mathbf{r}_a|) \right] \tag{4}$$

$$\left\langle \nabla^2 \phi \right\rangle_a = \frac{2d}{\lambda n_0} \sum_{b \neq a} \left[(\phi_b - \phi_a) w(|\mathbf{r}_b - \mathbf{r}_a|) \right] \tag{5}$$

Here, ϕ and $\mathbf{u}$ are scholar and vector variables, $\mathbf{r}$ is the position vector, $w(r) = r_e/r - 1$ ($0<r \leq r_e$) is a weight function, d is the dimensional number, and n_0 is the constant particle number density. The subscripts a and b denote the indices of the particle of interest and its neighboring particle. λ is a constant to cause the increase in statistical dispersion to conform to the analytical solution.

$$\lambda = \sum_{b \neq a} |\mathbf{r}_b - \mathbf{r}_a|^2 w(|\mathbf{r}_b - \mathbf{r}_a|) \Big/ \sum_{b \neq a} w(|\mathbf{r}_b - \mathbf{r}_a|) \tag{20}$$

These differential operators enable us to solve the continuity equation and the Navier-Stokes equation without a mesh. Unrealistic oscillation frequently appears in the pressure distribution, and numerical algorithms to suppress the pressure oscillation have been studied [87-93].

3.2 Applications of MPS method to molding of composites

MPS method has been applied to fluid engineering involving naval, civil and offshore engineering as well as micro-flow and biomechanics [94]. Although there are very few applications to composite materials, the Lagrangian nature is appropriate for molding analysis to investigate microstructure formation. However, a large-scale simulation is difficult due to the high calculation cost, and molding process has been predicted in a part of a component.

Yashiro et al. [95] presented a numerical approach for predicting the injection molding process of short-fiber reinforced plastics using MPS method. The thermoplastic resin was assumed to be an incompressible viscous fluid, and the fibers were modeled as rigid bodies by connecting some particles. Motion of rigid fibers was then coupled weakly with viscous flow. The explicit model could track individual fibers, and this characteristic was useful to discuss

mechanism of fiber orientation. This approach was verified further by comparing predictions with theories and experiments [96]. Velocity distribution in a straight path coincided with the analytical solution of the Poiseuille flow, and distribution of the velocity relative to that of the flow front exhibited a fountain flow. Prediction of the fiber orientation angle in a simple shear flow agreed with the Jeffery's solution. Correspondence between this approach and the orientation distribution function [97] was also discussed. Furthermore, prediction of fiber orientation distribution in a T-shaped bifurcation agreed well with experiment results. The series of validations demonstrated that this approach had capability to quantitatively evaluate the molding process of composite materials. Rigid fibers are good approximation for short fibers but are not appropriate for deformable long fibers.

Matsutani et al. [98] applied the MPS simulation with rigid fibers to three-dimensional flow of a stampable thermoplastic composite sheet, and addressed reduction of calculation cost through four improvements, namely, implicit calculation of velocity, simplified pressure calculation, parallel computing, and parameterized walls. Compression molding of a circular plate and a rib structure was predicted successfully. Shino et al. [99] proposed an anisotropic fluid model for compression molding of the multi-layer long-fiber-reinforced thermoplastic. A composite sheet was assumed to be homogeneous fluid having anisotropic viscosity. Compression of four stacked layers resulted in a deformation state varied by each layer due to the anisotropy.

Okabe et al. [100] analyzed microscopic resin flow in a fiber bundle, which is a part of RTM. Three phases (fibers, resin and air) were modeled explicitly to clarify the mechanism of air entrapments in a fiber bundle. Since capillary effect was significant in the microscopic flow between fibers, the surface tension was introduced as an external force. A Lenard-Jones-type surface tension potential was verified by droplet collapse and capillary flow. Microscopic flow

in a fiber bundle was then predicted, and the formation of micro-voids was investigated.

A potential of surface tension for MPS method was found in literature [101], which was similar to that introduced into SPH [102]. This surface tension model was confirmed by several numerical analyses [103,104]. Figure 2 presents resin flow into (and between) some fiber bundles using the surface tension model [101] with two contact angles θ. Resin particles were drawn to fibers in the case of high wettability, and the center bundle was almost filled with resin when θ=60°. In contrast, poor wettability caused repulsive interaction between resin particles and fiber particles, and resin was difficult to flow into a fiber bundle. In such a case, resin passed faster between bundles than passing through a bundle, and finally, many air particles remained in the bundle when θ=120°. These microscopic flow simulations reproduced the experimental knowledge on micro-void formation [105].

3.3 Summary

MPS method facilitates modeling of inhomogeneous fluid like fiber suspension. Their microstructure can be modeled explicitly without a homogenized constitutive law. More specifically, this modeling approach represents all inclusions and resin by an assembly of particles, and automatically analyzes the interaction between an inclusion and resin and between inclusions through the coupling scheme. Non-Newtonian nature of resin can be considered by assigning local viscosity as a function of the shear rate and temperature to a particle. It is noted that MPS method is applicable to other problems like heat transfer and solids, since it provides a discretized expression of a general differential equation as with SPH. A more realistic molding simulation is thus possible. However, when solidified resin is represented by particles, bumpy surface will be generated on a mold, resulting in a disturbed flow. Unrealistic oscillation of pressure is also a significant issue to obtain quantitative results. Moreover, high

calculation cost is a severe limitation for a molding simulation of a full-scale component. Therefore, prediction of whole molding process of composite components will need further development.

4. Discrete element method (DEM)

4.1 Fundamental concept

DEM was proposed to analyze motion of discontinuum like powders and sand particles [106,107]. This method is often referred to as distinct element method in civil engineering. Elements (i.e., particles) are assumed to be rigid, and motion of each particle is calculated based on Newton's second law. The force and torque acting on a particle are calculated by considering all particles contacting with the particle of interest. A rigid particle allowed to overlap slightly with other particles, and the contact force is calculated from the overlap by the Voigt model having a spring and a dashpot connected in parallel. There are several models for the spring and the dashpot [108-113], and the influence of the material properties for the contact model was described in a review article [114].

Spherical particles have been frequently used because of easy handling of contact. Ellipsoid and polyhedral particles have also been developed [115]. An arbitrary shape is represented by the clumped particle model, in which spherical particles are connected together rigidly [116-118]. Naturally, this model provides an approximate shape consisting of some arcs.

It is noted that DEM is a numerical method for assembly of discrete particles, not a discretization method for differential equations like SPH and MPS method. The numerical algorithm solving the equation of motion for the individual particles in a time marching manner is similar to the molecular dynamics.

4.2 Applications

DEM has been employed to predict dynamic behavior of particulate systems with weak bonds, e.g., particle packing and particle flow. Applications of DEM can be found in a wide range of engineering such as solid mixing, die filling, powder conveying, milling, and fluidized bed [119-121]. Analysis of motion of balls in a ball mill (Fig. 3) is a typical work of DEM (e.g., [122]). The balls passed through approximately constant paths due to the two dimensional simulation. In the actual milling process, powders will be crushed and stuck to balls, resulting in a change in the material properties of the contact model used. A large-scale practical simulation of bead milling has been presented recently using coupled DEM-MPS method for solid-fluid multiphase flow [123].

4.2.1 Concrete

Asphalt concrete is an inhomogeneous material that includes aggregate in cement. Many applications of DEM to concrete can be found in literature and a review [124]. Macroscopic deformation and failure of concrete will be predicted by homogenizing the material and calibrating properties of the spring and dashpot (e.g., [125,126]). This section, however, focuses on some studies that represents explicitly the inhomogeneous nature.

In the very early work [127], only gravel was modeled by particles, and mortar was assumed to be nonlinear springs. This approach could consider not only contacts between gravel particles but also binding effect of mortar. This work was applied to local damage prediction in concrete structures due to impact loading [128].

In recent years, both of aggregate and cement have been modeled by particles, and an arbitrary shape of aggregate has been represented by tying up some particles [129-131]. Inter-particle contacts have been treated by a brittle linear spring or a bilinear softening spring.

Influence of aggregate on macroscopic material properties and failure was investigated through this explicit modeling approach. Kim et al. [132,133] implemented a bilinear cohesive zone model into the DEM framework to predict crack initiation and propagation in asphalt concrete. Crack propagation in a homogeneous disk-shaped compact tension specimen (i.e., a dense-graded asphalt concrete) agreed well with an experiment result. Furthermore, an image-based inhomogeneous DEM model, in which large aggregate was represented explicitly by some particles tied together, was constructed to simulate microscopic fracture process.

4.2.2 Powder compaction and sintering of particulate composites

The four major mechanisms of densification in powder compaction are rearrangement, plastic deformation, creep, and diffusional flow. DEM is an approach that allows all of the above mechanisms. Contact models, i.e., relationship between the overlap of two particles and the repulsive force, have been investigated for a pure material to achieve valid behavior up until high compaction rate (e.g., [134,135]). These models have been applied to metal-matrix composites (MMCs) and CMCs. Martin and Bouvard [136] analyzed 3D compaction of mixture of soft and hard particles to study the effect of hard-particle sliding on the compaction behavior considering viscoplastic deformation. The friction coefficient of hard-hard particle contacts played a significant role in development of a load-carrying network by hard particles, which would prevent deformation of soft phase. A decohesion model was introduced into DEM to analyze the unloading behavior (spring-back) of powder compacts [137]. The effect of bimodal size distribution on compaction of spherical metallic powders was also studied [138]. The initially-obtained high relative density achieved compaction by a strain smaller than uniform size packing. This result is beneficial for control of part dimensions both at the compaction stage (unloading) and the post-compaction process (sintering). Skrinjar and Larsson [139]

analyzed cold compaction of composite powders with size difference. When the volume fraction of large and hard particles was high, predictions suggested a much stiffer response of the powder compound than theoretical ones. Methods were also presented for determining pore distributions from the final particle arrangement [140].

Sintering simulations have been performed by using a contact force model that describes the sintering process. Olmos et al. [141] analyzed sintering behavior of metal powders mixed with ceramic inclusions. Sintering contact models were assumed that mass transport mechanisms are governed by grain boundary diffusion. Metal-metal contacts were represented by a constitutive law that considered diffusion and surface energy effects in the sintering process, while ceramic-ceramic contacts and ceramic-metal contacts were assumed to be elastic and viscous. Yan et al. [142] generalized this sintering contact model for multi-size particle mixtures and investigated the effect of volume fraction, size and homogeneity of rigid non-sintering inclusions on the densification behavior. The improved model was applied to microstructure evolution during co-sintering of ultrathin multilayer ceramic capacitors [143].

4.2.3 Mechanical behavior and damage accumulation in composites

Mechanical properties and damage accumulation in composite materials have been evaluated by DEM within the last decade, because contact/parallel bond models [107,108] and cohesive contact models [132,144] have been developed for materials under tensile loading. Here, the contact bond can carry only force, while the parallel bond can carry both force and torque. These models along with the particulate nature of DEM enables reinforcement/matrix explicit modeling.

Wittel's works [145,146] are the first attempts that predicted crack onset and accumulation in fiber reinforced plastics (FRPs) by DEM. A disordered spring network model was proposed

to study accumulation of transverse cracks in cross-ply laminates in the fabrication process of carbon/carbon composites [145] and in the tensile loading process [146]. Random breaking thresholds were assigned to springs to handle stochastic nature of transverse cracks.

Potyondy and Cundall [107] proposed a bonded-particle model and implemented it into a commercial DEM code. Although this model was proposed for rocks, it is applicable to various materials subjected to tensile loading. There are two modeling approaches for composite materials. One represents high-content reinforcements by particles and takes into account the effect of surrounding matrix by the bond model [147]. The other represents both of reinforcements and matrix by particles and applies appropriate bond models to links between reinforcements, between matrices, and between a reinforcement and a matrix [148]. The former will provide reasonable macroscopic behavior with low calculation cost, but efforts will be required for calibration of the bond model. The latter will take a higher calculation cost but can evaluate microscopic properties between reinforcements and matrix. Composite materials have been modeled by the latter approach.

Ye and his colleagues focused on various inhomogeneity in FRPs and performed several failure analyses, namely, cracking in a 90° ply [149], microbond test [150], interlaminar toughness evaluation [151], and generation of transverse cracks and delamination in a cross-ply laminate [152]. The microstructure was modeled by employing different constitutive laws and material parameters for different constituents and interfaces. A contact softening model which was similar to the cohesive zone model was used to account for the matrix-matrix bonds, fiber/matrix interfaces and 0°/90° ply interfaces.

Curvy warp yarns as well as fibers and matrix in weft yarns in woven composites were modeled explicitly [153,154]. Short-fiber reinforced cementitious composites were modeled in a similar manner to investigate influence of fibers on the cracking path and the macroscopic

stress-strain relation [155]. The contact bond model has been applied to adhesion between two different materials such as metal/foam core sandwich panels [156] and concrete/FRP bonded joints [157,158] for predictions of disbond onset.

Most recently, mechanical properties and damage extension of composite materials have been analyzed by considering the representative elementary volume (REV). Haddad et al. [159] developed DEM-based REV of a ceramic-particle/epoxy composite and compared elastic properties with those obtained by other numerical simulations and analytical solutions. Ismail et al. [160] predicted accumulation of micro-cracks and formation of a ply-crack by using 2D-REV of unidirectional FRPs under transverse tension. Ismail et al. [161] proposed an approach to develop DEM-based REV of a transverse ply with considering fiber diameter variation and random allocation of fibers. Maheo et al. [162] modeled 3D-REV of a single fiber surrounded by matrix to treat local damage like debonding. Le et al. [163] improved the contact model for interfacial debonding used in Ref. [162] and predicted growth of a single crack in a multi-fiber-composite model under transverse tension.

4.2.4 Other topics on composite materials

Machining of CFRPs is difficult due to the inhomogeneous and anisotropic nature and to the abrasive behavior of carbon fibers. Process of orthogonal cutting have been analyzed by FEM to clarify the mechanism of fiber cutting, chip ejection and damage extension [164,165], although it is rarely used in practical machining of FRPs. Taking advantage of easy handling of fracture at an arbitrary position, orthogonal cutting of a unidirectional CFRP plate was simulated [166]. DEM prediction agreed well with experimental observations and described faithfully the mechanisms of composite cutting. DEM simulation has possibility of predicting abrasive wear of a cutting tool by representing it by particles.

Thermal conductivity of composite materials has been predicted with taking into account their microstructures [167,168]. In these studies, fabrication of the material was first analyzed by DEM, and REV was extracted from the obtained particle arrangement. This REV was discretized by finite elements, and the overall thermal conductivity was analyzed by FEM. This approach can investigate influence of microstructure and contact state on macroscopic material properties.

DEM has recently been applied to multi-scale analysis [169,170]. The explicit modeling capability and various particle linking models facilitate microscale and meso-scale analyses. Passing material properties between different scales will be a tough challenge in multi-scale analysis, since DEM usually requires calibration of contact models to reproduce dynamic response of materials.

4.3 Summary

DEM has the following inherent advantages from its theoretical development: (1) the discrete nature of a material can be modeled explicitly by particles; (2) the calculation algorithm is robust over changing contacts and moving boundaries; (3) large deformation and frictional sliding between particles are handled routinely. Good applications can thus be found in dynamic motion of particulate systems with weak bonds. DEM has also been applied to materials under tensile loading by using improved contact models. Since an arbitrary pair of particles satisfying a failure criterion breaks automatically, DEM is useful for predicting fracture of a material with strong inhomogeneity. More specifically, DEM has no need to insert a special contact representing material failure into a specified position just like cohesive elements in FEM. Ease of image-based modeling [132,133,171] is the other advantage for composite materials.

It should be noted that calibration of contact models is required to obtain adequate

macroscopic material response. Properties of contact models between particles are different from macroscopic material properties even for a pure material.

5. Concluding remarks

Three particle simulation methods, namely SPH, MPS and DEM are introduced. These methods have the common advantages of easy preprocess for a complex-shaped object and easy handling of large deformation and moving discontinuity (e.g., motion of crack tips and free surfaces). The major drawback is significantly high calculation cost compared with FEM. With expanding use of composite materials, our composite community has to overcome wide range of engineering challenges, and the particle simulation methods will be appropriate for a part of them. This review article described approaches for modeling composite materials based on particles. Characteristics of the methods are summarized as follows.

- SPH is a dynamic simulation method for continua. The interpolation equation to represent spatial distribution and its differential expression enables analyses of various phenomena described by differential equations. Difficulty in defining a clear boundary is a drawback for explicit modeling of inhomogeneous materials. The scale of heterogeneity in SPH simulations is mostly a lamina, and effects of microstructure have been considered in constitutive laws. In practical fluid-solid interaction problems, SPH has been applied only to fluid, and FEM has been used to analyze dynamic response of composite structures.
- MPS method is applicable to inhomogeneous fluid. Inclusions and voids can be modeled explicitly by particles. MPS method have thus been used for predicting molding process of composite materials to clarify mechanism of microstructure evolution. Non-Newtonian nature and surface tension of resin can be handled easily. Unrealistic pressure oscillation is an issue for quantitative evaluation.

- DEM is a dynamic simulation method for discontinua. DEM is basically appropriate for particulate systems like powders and sands, but it has been applied to solids under tension by using various contact models. Because DEM facilitates modeling of an inhomogeneous material and representating fracture at an arbitrary point, it has recently been used to predict onset and accumulation of microscopic damage in FRPs. Calibration of contact models is required to obtain adequate macroscopic responses.

These three methods are useful for special phenomena and have several difficult issues such as their high calculation cost. It should be noted that they are not substitutes for FEM.

Acknowledgement

The author thanks Dr. Akinori Yoshimura (Japan Aerospace Exploration Agency) for his cooperation in the soft-body impact tests and DEM simulation coding.

References

[1] Gay D. Composite Materials: Design and Applications, Third Edition. CRC Press, 2014.

[2] Monaghan JJ. Smoothed particle hydrodynamics. Annu Rev Astron Astrophys 1992; 30:543-574.

[3] Monaghan JJ. Smoothed particle hydrodynamics. Rep Prog Phys 2005; 68:1703-1759.

[4] Liu MB, Liu GR. Smoothed particle hydrodynamics (SPH): an overview and recent developments. Arch Comput Methods Eng 2010; 17:25-76.

[5] Belytschko T, Lu YY, Gu L. Element-free Galerkin methods. Int J Numer Meth Eng 1994; 37:229-256.

[6] Lu YY, Belytschko T, Gu L. A new implementation of the element free Galerkin method. Comput Meth Appl Mech. Eng 1994; 113:397-414.

[7] Dolbow J, Belytschko T. An introduction to programming the meshless element free Gaalerkin method. Arc Comput Method Eng 1998; 5:207-241.

[8] Liu WK, Jun S, Zhang YF. Reproducing kernel particle methods. Int J Numer Meth Fluids

1995; 20:1081-1106.

[9] Liu WK, Jun S, Lit S, Adee J, Belytschko T. Reproducing kernel particle methods for structural dynamics. Int J Numer Meth Eng 1995; 38:1655-1679.

[10] Atluri SN, Zhu T. A new meshless local Petrov-Galerkin (MLPG) approach in computational mechanics. Comput Mech 1998; 22:117-127.

[11] Atluri SN, Zhu T-L. The meshless local Petrov-Galerkin (MLPG) approach for solving problems in elasto-statics. Comput Mech 2000; 25:169-179.

[12] Atluri SN, Shen S. The meshless local Petrov-Galerkin (MLPG) method: A simple & less-costly alternative to the finite element and boundary element methods. CMES: Comput Model Eng Sci 2002; 3:11-51.

[13] Sladek J, Stanak P, Han Z-D, Sladek V, Atluri SN. Applications of the MLPG method in engineering & sciences: a review. CMES: Comput Model Eng Sci 2013; 92:423-475.

[14] Liew KM, Zhao X, Ferreira AJM. A review of meshless methods for laminated and functionally graded plates and shells. Compos Struct 2011; 93:2031-2041.

[15] Nguyen VP, Rabczuk T, Bordas S, Duflot M. Meshless methods: A review and computer implementation aspects. Math Comput Simul 2008; 79:763-813.

[16] Gingold RA, Monaghan JJ. Smoothed particle hydrodynamics: theory and application to non-spherical stars. Mon Not R Astr Soc 1977; 181:375-389.

[17] Lucy LB. A numerical approach to the testing of the fission hypothesis. Astron J 1977; 82:1013-1024.

[18] Monaghan JJ. Simulating free surface flows with SPH. J Comput Phys 1994; 110:399-406.

[19] Takeda H, Miyama SM, Sekiya M. Numerical simulation of viscous flow by smoothed particle hydrodynamics. Prog Theor Phys 1994; 92:939-960.

[20] Morris JP, Fox PJ, Zhu Y. Modeling low Reynolds number incompressible flows using SPH. J Comput Phys 1997; 136:214-226.

[21] Lee ES, Moulinec C, Xu R, Violeau D, Laurence D, Stansby P. Comparisons of weakly compressible and truly incompressible algorithms for the SPH mesh free particle method. J Comput Phys 2008; 227:8417-8436.

[22] Szewc K, Pozorski J, Minier JP. Analysis of the incompressibility constraint in the smoothed particle hydrodynamics method. Int J Numer Meth Eng 2012; 92:343-369.

[23] Libersky LD, Petschek AG, Carney TC, Hipp JR, Allahdadi FA. High strain Lagrangian

hydrodynamics: a three dimensional SPH code for dynamic material response. J Comput Phys 1993; 109:67-75.

[24] Benz W, Asphaug E. Simulations of brittle solids using smooth particle hydrodynamics. Comput Phys Commun 1995; 87:253-265.

[25] Johnson GR, Stryk RA, Beissel SR. SPH for high velocity impact computations. Comput Meth Appl Mech Eng 1996; 139:347-373.

[26] Randles PW, Libersky LD. Smoothed particle hydrodynamics: some recent improvements and applications. Comput Meth Appl Mech Eng 1996; 139:375-408.

[27] Gray JP, Monaghan JJ, Swift RP. SPH elastic dynamics. Comput Meth Appl Mech Eng 2001; 190:6641-6662.

[28] Monaghan JJ. Shock simulation by the particle method SPH. J Computat Phys 1983; 52:374-389.

[29] Swegle JW, Hicks DL, Attaway SW. Smoothed particle hydrodynamics stability analysis. J Comput Phys 1995; 116:123-134.

[30] Dyka CT, Ingel RP. An approach for tension instability in smoothed particle hydrodynamics (SPH). Comput Struct 1995; 57:573-580.

[31] Dyka CT, Randles PW, Ingel RP. Stress points for tension instability in SPH. Int J Numer Meth Eng 1997; 40:2325-2341.

[32] Monaghan JJ. SPH without a tensile instability. J Comput Phys 2000; 159:290-311.

[33] Cleary PW, Prakash M, Ha J, Stokes N, Scott C. Smooth particle hydrodynamics: status and future potential. Prog Comput Fluid Dynam 2007; 7:70-90.

[34] Chen JK, Allahdadi FA, Carney TC. High-velocity impact of graphite/epoxy composite laminates. Compos Sci Technol 1997; 57:1369-1379.

[35] Medina DF, Chen JK. Three-dimensional simulations of impact induced damage in composite structures using the parallelized SPH method. Compos Part A 2000; 31:853-860.

[36] Hayhurst CJ, Hiermaier SJ, Clegg RA, Riedel W, Lambert M. Development of material models for Nextel and Kevlar-epoxy for high pressures and strain rates. Int J Impact Eng 1999; 23:365-376.

[37] White DM, Taylor EA, Clegg RA. Numerical simulation and experimental characterisation direct hypervelocity impact on a spacecraft hybrid carbon fibre/Kevlar composite structure. Int J Impact Eng 2003; 29:779-790.

[38] Chen JK, Medina DF. The effects of projectile shape on laminated composite perforation. Compos Sci Technol 1998; 58:1629-1639.

[39] Shintate K, Sekine H. Numerical simulation of hypervelocity impacts of a projectile on laminated composite plate targets by means of improved SPH method. Compos Part A 2004; 35:683-692.

[40] Yashiro S, Ogi K, Yoshimura A, Sakaida Y. Characterization of high-velocity impact damage in CFRP laminates: Part II - prediction by smoothed particle hydrodynamics. Compos Part A 2014; 56:308-318.

[41] Lee M, Yoo YH. Analysis of ceramic/metal armour systems. Int J Impact Eng 2001; 25:819-829.

[42] Ohtani K, Numata D, Kikuchi T, Sun M, Takayama K, Togami K. A study of hypervelocity impact on cryogenic materials. Int J Impact Eng 2006; 33:555-565.

[43] Lee M. Analysis of high-explosive fragmenting shell impact into spaced plates. Int J Impact Eng 2006; 33:364-370.

[44] De Vuyst T, Vignjevic R, Campbell JC. Coupling between meshless and finite element methods. Int J Impact Eng 2005; 31:1054-1064.

[45] Hayhurst CJ, Livingstone IHG, Clegg RA, Destefanis R, Faraud M. Ballistic limit evaluation of advanced shielding using numerical simulations. Int J Impact Eng 2001; 26:309-320.

[46] Clegg RA, White DM, Riedel W, Harwick W. Hypervelocity impact damage prediction in composites: Part I-material model and characterization. Int J Impact Eng 2006; 33:190-200.

[47] Riedel W, Nahme H, White DM, Clegg RA. Hypervelocity impact damage prediction in composites: Part II-experimental investigations and simulations. Int J Impact Eng 2006; 33:670-680.

[48] Taylor EA, Glanville JP, Clegg RA, Turner RG. Hypervelocity impact on spacecraft honeycomb: hydrocode simulation and damage laws. Int J Impact Eng 2003; 29:691-702.

[49] Wicklein M, Ryan S, White DM, Clegg RA. Hypervelocity impact on CFRP: Testing, material modelling, and numerical simulation. Int J Impact Eng 2008; 35:1861-1869.

[50] Buyuk M, Kurtaran H, Marzougui D, Kan CD. Automated design of threats and shields under hypervelocity impacts by using successive optimization methodology. Int J Impact Eng 2008; 35:1449-1458.

[51] Son BJ, Yoo J, Lee M. Optimal design of a composite space shield based on numerical simulations. J Mech Sci Technol 2015; 29:5299-5308.

[52] Cherniaev A, Telichev I. Numerical simulation of impact damage induced by orbital debris on shielded wall of composite overwrapped pressure vessel. Appl Compos Mater 2014; 21:861-884.

[53] Cherniaev A, Telichev I. Meso-scale modeling of hypervelocity impact damage in composite laminates. Compos Part B 2015; 74:95-103.

[54] Hou JP, Ruiz C. Soft body impact on laminated composite materials. Compos Part A 2007; 38:505-515.

[55] Heimbs S. Computational methods for bird strike simulations: A review. Comput Struct 2011; 89:2093-2112.

[56] Johnson AF, Holzapfel M. Modelling soft body impact on composite structures. Compos Struct 2003; 61:103-113.

[57] McCarthy MA, Xiao JR, McCarthy CT, Kamoulakos A, Ramos J, Gallard JP, Melito V. Modelling of bird strike on an aircraft wing leading edge made from fibre metal laminates - Part 2: modelling of impact with SPH bird model. Appl Compos Mater 2004; 11:317-340.

[58] McCarthy MA, Xiao JR, McCarthy CT, Kamoulakos A, Ramos J, Gallard JP, Melito V. Modelling bird impacts on an aircraft wing - Part 2: Modelling the impact with an SPH bird model. Int J Crashworthiness 2005; 10:51-59.

[59] Kermanidis Th, Labeas G, Sunaric M, Ubels L. Development and validation of a novel bird strike resistant composite leading edge structure. Appl Comos Mater 2005; 12:327-353.

[60] Kermanidis Th, Labeas G, Sunaric M, Johnson AF, Holzapfel M. Bird strike simulation on a novel composite leading edge design. Int J Crashworthiness 2006; 11:189-201.

[61] Johnson AF, Holzapfel M. Numerical prediction of damage in composite structures from soft body impacts. J Mater Sci 2006; 41:6622-6630.

[62] Georgiadis S, Gunnion AJ, Thomson RS, Cartwright BK. Bird-strike simulation for certification of the Boeing 787 composite moveable trailing edge. Compos Struct 2008; 86:258-268.

[63] Guida M, Marulo F, Meo M, Grimaldi A, Olivares G. SPH - Lagrangian study of bird impact on leading edge wing. Compos Struct 2011; 93:1060-1071.

[64] Grimaldi A, Sollo A, Guida M, Marulo F. Parametric study of a SPH high velocity impact analysis - A birdstrike windshield application. Compos Struct 2013; 96:616-630.

[65] Halpin JC. Private communication. February 2016.

[66] Seddon CM, Moatamedi M. Review of water entry with applications to aerospace structures. Int J Imact Eng 2006; 32:1045-1067.

[67] Fasanella EL, Jackson KE. Water impact test and simulation of a composite energy absorbing fuselage section. J Am Helicopter Soc 2005; 50:150-164.

[68] Panciroli R, Abrate S, Minak G, Zucchelli A. Hydroelasticity in water-entry problems: Comparison between experimental and SPH results. Compos Struct 2012; 94:532-539.

[69] Poodts E, Panciroli R, Minak G. Design rules for composite sandwich wakeboards. Compos Part B 2013; 44:628-638.

[70] Anghileri M, Castelletti L-ML, Francesconi E, Milanese A, Pittofrati M. Survey of numerical approaches to analyse the behavior of a composite skin panel during a water impact. Int J Impact Eng 2014; 63:43-51.

[71] Artero-Guerrero JA, Pernas-Sánchez J, López-Puente J, Varas D. On the influence of filling level in CFRP aircraft fuel tank subjected to high velocity impacts. Compos Struct 2014; 107:570-577.

[72] Ogierman W, Kokot G. Numerical analysis of the influence of the blast wave on the composite structure. Mechanika 2014; 20:147-152.

[73] Comas-Cardona S, Groenenboom P, Binetruy C, Krawczak P. A generic mixed FE-SPH method to address hydro-mechanical coupling in liquid composite moulding processes. Compos Part A 2005; 36:1004-1010.

[74] Hall J, Qamar IPS, Rendall TCS, Trask RS. A computational model for the flow of resin in self-healing composites. Smart Mater Struct 2015; 24:037002.

[75] Deeb R, Karihaloo BL, Kulasegaram S. Reorientation of short steel fibres during the flow of self-compacting concrete mix and determination of the fibre orientation factor. Cement Concrete Res 2014; 56:112-120.

[76] Wang X, Zhang H, Zheng L, Wei J. Development of a mesoscopic particle model for synthesis of uranium-ceramic nuclear fuel. Int J Heat Mass Trans 2009; 52:5141-5151.

[77] Chen Y, Kulasegaram S. Numerical modelling of fracture of particulate composites using SPH method. Comput Mater Sci 2009; 47:60-70.

[78] Lin J, Naceur H, Laksimi A, Coutellier D. On the implementation of a nonlinear shell-

based SPH method for thin multilayered structures. Compos Struct 2014; 108:905-914.

[79] Chen JK, Beraun JE, Jih CJ. An improvement for tensile instability in smoothed particle hydrodynamics. Comput Mech 1999; 23:279-287.

[80] Chen JK, Beraun JE, Carney TC. A corrective smoothed particle method for boundary value problems in heat conduction. Int J Numer Meth Eng 1999; 46:231-252.

[81] Lin J, Naceur H, Coutellier D, Abrate S. Numerical modeling of the low-velocity impact of composite plates using a shell-based SPH method. Meccanica 2015; 50:2649-2660.

[82] Yashiro S, Okabe T. Smoothed particle hydrodynamics in a generalized coordinate system with a finite-deformation constitutive model. Int J Numer Meth Eng 2015; 103:781-797.

[83] Ikawa T, Yashiro S, Okabe T, Sakaida Y. Smoothed particle hydrodynamics in generalized coordinate system and its application to bird strike simulation. Proc. 6th Japan Conference on Composite Materials (JCCM-6), March 2015, No. 1A-12. (in Japanese)

[84] Koshizuka S, Oka Y. Moving particle semi-implicit method for fragmentation of incompressible fluid. Nucl Sci Eng 1996; 123:421-434.

[85] Koshizuka S, Nobe A, Oka Y. Numerical analysis of breaking waves using the moving particle semi-implicit method. Int J Numer Meth Fluids 1998; 26:751-769.

[86] Chikazawa Y, Koshizuka S, Oka Y. A particle method for elastic and visco-plastic structures and fluid-structure interactions. Comput Mech 2001; 27:97-106.

[87] Tanaka M, Masunaga T. Stabilization and smoothing of pressure in MPS method by Quasi-Compressibility. J Comput Phys 2010; 229:4279-4290.

[88] Kondo M, Koshizuka S. Suppressing the numerical oscillations in moving particle semi-implicit method. Trans Jpn Soc Comput Eng Sci 2008; No. 20080015. (in Japanese)

[89] Hibi S, Yabushita K. A study on reduction of unusual pressure fluctuation of MPS method. J Kansai Soc Naval Architects 2004; 241:125-131. (in Japanese)

[90] Sueyoshi M. Validation of a numerical code by a particle method for violent free surface problems. Int J Offshore Polar Eng 2006; 16:261-267.

[91] Kondo M, Koshizuka S. Improvement of stability in moving particle semi-implicit method. Int J Numer Meth Fluids 2011; 65:638-654

[92] Khayyer A, Gotoh H. Modified moving particle semi-implicit methods for the prediction of 2D wave impact pressure. Coastal Eng 2009; 56:419-440.

[93] Khayyer A, Gotoh H. Enhancement of stability and accuracy of the moving particle semi-implicit method. J Comput Phys 2011; 230:3093-3118.

[94] Koshizuka S. Current Current achievements and future perspectives on particle simulation technologies for fluid dynamics and heat transfer. J Nucl Sci Technol 2011; 48:155-168.

[95] Yashiro S, Okabe T, Matsushima K. A numerical approach for injection molding of short-fiber-reinforced plastics using a particle method. Adv Compos Mater 2011; 20:503-517.

[96] Yashiro S, Sasaki H, Sakaida Y. Particle simulation for predicting fiber motion in injection molding of short-fiber-reinforced composites. Compos Part A 2012; 43:1754-1764.

[97] Advani SG, Tucker CL. The use of tensors to describe and predict fiber orientation in short fiber composites. J Rheol 1987; 31:751-784.

[98] Matsutani H, Taketa I, Hashimoto M, Hirano N, Okabe T. Flow simulation of thermoplastic stampable sheet using particle method. J Jpn Soc Compos Mater 2014; 40:227-237. (in Japanese)

[99] Shino R, Tamai T, Koshizuka S, Maki A, Ishikawa T. Press molding analysis with anisotropic high viscosity fluid model using particle method. Proc. 7th Japan Conference on Composite Materials (JCCM-7), March 2016, No. 1C-09. (in Japanese)

[100] Okabe T, Matsutani H, Honda T, Yashiro S. Numerical simulation of microscopic flow in a fiber bundle using the moving particle semi-implicit method. Compos Part A 2012; 43:1765-1774.

[101] Kondo M, Koshizuka S, Takimoto M. Surface tension model using inter-particle potential force in moving particle semi-implicit method. Trans Jpn Soc Comput Eng Sci 2007; No. 20070021. (in Japanese)

[102] Tartakovsky A, Meakin P. Modeling of surface tension and contact angles with smoothed particle hydrodynamics. Phys Rev E 2005; 72:026301.

[103] Natsui S, Soda R, Kon T, Ueda S, Kano J, Inoue R, Ariyama T. Wettability model considering three-phase interfacial energetics in particle method. Mater Trans 2012; 53:662-670.

[104] Kon T, Natsui S, Ueda S, Inoue R, Ariyama T. Influence of physical properties of melt on liquid dripping in packed bed analyzed by MPS method. ISIJ Int 2013; 53:590-597.

[105] Rohatgi V, Patel N, Lee LJ. Experimental investigation of flow-induced microvoids during impregnation of unidirectional stitched fiberglass mat. Polym Compos 1996; 17:161-170.

[106] Cundall PA, Strack ODL. A discrete numerical model for granular assemblies.

Geotechnique 1979; 29:47-65.

[107] Potyondy DO, Cundall PA. A bonded-particle model for rock. Int J Rock Mech Min Sci 2004; 41:1329-1364.

[108] Zhu HP, Zhou ZY, Yang RY, Yu AB. Discrete particle simulation of particulate systems: Theoretical developments. Chem Eng Sci 2007; 62:3378-3396.

[109] Langston PA, Tüzün U, Heyes DM. Discrete element simulation of granular flow in 2D and 3D hoppers: dependence of discharge rate and wall stress on particle interactions. Chem Eng Sci 1995; 50:967-987.

[110] Zhou YC, Wright BD, Yang RY, Xu BH, Yu AB. Rolling friction in the dynamic simulation of sandpile formation. Physica A 1999; 269:536-553.

[111] Walton OR. Numerical simulation of inclined chute flows of monodisperse, inelastic, frictional spheres. Mech Mater 1993; 16:239-247.

[112] Kruggel-Emden H, Simsek E, Rickelt S, Wirtz S, Scherer V. Review and extension of normal force models for the Discrete Element Method. Powder Technol 2007; 171:157-173.

[113] Luding S. Cohesive, frictional powders: contact models for tension. Granul Mater 2008; 10:235-246.

[114] Paulick M, Morgeneyer M, Kwade A. Review on the influence of elastic particle properties on DEM simulation results. Powder Technol 2015; 283:66-76.

[115] Lu G, Third JR, Müller CR. Discrete element models for non-spherical particle systems: From theoretical developments to applications. Chem Eng Sci 2015; 127:425-465.

[116] Cho N, Martin CD, Sego DC. A clumped particle model for rock. Int J Rock Mech Min Sci 2007; 44:997-1010.

[117] Markauskas D, Kačianauskas R, Džiugys A, Navakas R. Investigation of adequacy of multi-sphere approximation of elliptical particles for DEM simulations. Granul Matter 2010; 12:107-123.

[118] Samiei K, Berhe G, Peters B. Numerical prediction of the bulk density of granular particles of different geometries. KONA Powder Part J 2014; 31:265-270.

[119] Zhu HP, Zhou ZY, Yang RY, Yu AB. Discrete particle simulation of particulate systems: A review of major applications and findings. Chem Eng Sci 2008; 63:5728-5770.

[120] Weerasekara NS, Powell MS, Cleary PW, Tavares LM, Evertsson M, Morrison RD, Quist J, Carvalho RM. The contribution of DEM to the science of comminution. Powder

Technol 2013; 248:3-24.

[121] Sakai M. How should the discrete element method be applied in industrial systems?: A review. KONA Powder Part J 2016; 33:169-178.

[122] Kano J, Chujo N, Saito F. A method for simulating the three-dimensional motion of balls under the presence of a powder sample in a tumbling ball mill. Adv Powder Technol 1997; 8:39-51.

[123] Yamada Y, Sakai M. Lagrangian–Lagrangian simulations of solid–liquid flows in a bead mill. Powder Technol 2013; 239:105-114.

[124] Liu Y, You Z, Li L, Wang W. Review on advances in modeling and simulation of stone-based paving materials. Constr Build Mater 2013; 43:408-417.

[125] Hentz S, Donzé FV, Daudeville L. Discrete element modelling of concrete submitted to dynamic loading at high strain rates. Comput Struct 2004; 82:2509-2524.

[126] Shiu W, Donzé FV, Daudeville L. Penetration prediction of missiles with different nose shapes by the discrete element numerical approach. Comput Struct 2008; 86:2079-2086.

[127] Meguro K, Hakuno M. Fracture analyses of concrete structures by the modified distinct element method. Struct Eng Earthq Eng 1989; 6:283s-294s.

[128] Kusano N, Aoyagi T, Aizawa J, Ueno H, Morikawa H, Kobayashi N. Impulsive local damage analyses of concrete structure by the distinct element method. Nucl Eng Des 1992; 138:105-110.

[129] Azevedo NM, Lemos JV, de Almeida JR. Influence of aggregate deformation and contact behavior on discrete particle modelling of fracture of concrete. Eng Fract Mech 2008; 75:1569-1586.

[130] Khanal M, Raghuramakrishnan R, Tomas J. Discrete element method simulation of effect of aggregate shape on fragmentation of particle composite. Chem Eng Tech 2008; 31:1526-1531.

[131] Liu Y, You Z, Zhao Y. Three-dimensional discrete element modeling of asphalt concrete: Size effects of elements. Constr Build Mater 2012; 37:775-782.

[132] Kim H, Wagoner MP, Buttlar WG. Simulation of fracture behavior in asphalt concrete using a heterogeneous cohesive zone discrete element model. J Mater Civil Eng 2008; 20:552-563.

[133] Kim H, Buttlar WG. Discrete fracture modeling of asphalt concrete. Int J Solids Struct 2009; 46:2593-2604.

[134] Martin CL, Bouvard D, Shima S. Study of particle rearrangement during powder compaction by the Discrete Element Method. J Mech Phys Solids 2003; 51:667-693.

[135] Harthong B, Jérier J-F, Dorémus P, Imbault D, Donzé F-V. Modeling of high-density compaction of granular materials by the Discrete Element Method. Int J Solids Struct 2009; 46:3357-3364.

[136] Martin CL, Bouvard D. Study of the cold compaction of composite powders by the discrete element method. Acta Mater 2003; 51:373-386.

[137] Martin CL. Unloading of powder compacts and their resulting tensile strength. Acta Mater 2003; 51:4589-4602.

[138] Martin CL, Bouvard D. Isostatic compaction of bimodal powder mixtures and composites. Int J Mech Sci 2004; 46:907-927.

[139] Skrinjar O, Larsson P-L. Cold compaction of composite powders with size ratio. Acta Mater 2004; 52:1871-1884.

[140] Sweeney SM, Martin CL. Pore size distributions calculated from 3-D images of DEM-simulated powder compacts. Acta Mater 2003; 51:3635-3649.

[141] Olmos L, Martin CL, Bouvard D. Sintering of mixtures of powders: Experiments and modelling. Powder Technol 2009; 190:134-140.

[142] Yan Z, Martin CL, Guillonc O, Bouvard D. Effect of size and homogeneity of rigid inclusions on the sintering of composites. Scr Mater 2013; 69:327-330.

[143] Yan Z, Martin CL, Guillon O, Bouvard D, Lee CS. Microstructure evolution during the co-sintering of Ni/BaTiO3multilayerceramic capacitors modeled by discrete element simulations. J Eur Ceram Soc 2014; 34:3167-3179.

[144] Delenne J-Y, Youssoufi MSE, Cherblanc F, Bénet J-C. Mechanical behaviour and failure of cohesive granular materials. Int J Numer Anal Methods Geomech 2004; 28:1577-1594.

[145] Wittel FK, Schulte-Fischedick J, Kun F, Kröplin B-H, Frieß M. Discrete element simulation of transverse cracking during the pyrolysis of carbon fibre reinforced plastics to carbon/carbon composites. Comput Mater Sci 2003; 28:1-15.

[146] Wittel FK, Kun F, Kröplin B-H, Herrmann HJ. A study of transverse ply cracking using a discrete element method. Comput Mater Sci 2003; 28:608-619.

[147] Wolff MFH, Salikov V, Antonyuk S, Heinrich S, Schneider GA. Three-dimensional discrete element modeling of micromechanical bending tests of ceramic–polymer composite materials. Powder Technol 2013; 248:77-83.

[148] Mohandesi JA, Refahi A, Meresht ES, Berenji S. Effect of temperature and particle weight fraction on mechanical and micromechanical properties of sand-polyethylene terephthalate composites: A laboratory and discrete element method study. Compos Part B 2011; 42:1461-1467.

[149] Sheng Y, Yang D, Tan Y, Ye J. Microstructure effects on transverse cracking in composite laminae by DEM. Compos Sci Technol 2010; 70:2093-2101.

[150] Yang D, Sheng Y, Ye J, Tan Y. Discrete element modeling of the microbond test of fiber reinforced composite. Comput Mater Sci 2010; 49:253-259.

[151] Yang D, Ye J, Tan Y, Sheng Y. Modeling progressive delamination of laminated composites by discrete element method. Comput Mater Sci 2011; 50:858-864.

[152] Yang D, Sheng Y, Ye J, Tan Y. Dynamic simulation of crack initiation and propagation in cross-ply laminates by DEM. Compos Sci Technol 2011; 71:1410-1418.

[153] Khattab A, Khattak MJ, Fadhi IM. Micromechanical discrete element modeling of fiber reinforced polymer composites. Polym Compos 2011; 32:1532-1540.

[154] Khattak MJ, Khattab A. Modeling tensile response of fiber-reinforced polymer composites using discrete element method. Polym Compos 2013; 34:877-886.

[155] Herrmann H, Eik M, Berg V, Puttonen J. Phenomenological and numerical modelling of short fibre reinforced cementitious composites. Meccanica 2014; 49:1985-2000.

[156] Zha X, Wan C, Fan Y, Ye J. Discrete element modeling of metal skinned sandwich composite panel subjected to uniform load. Comput Mater Sci 2013; 69:73-80.

[157] Biscaia HC, Micaelo R, Teixeira J, Chastre C. Numerical analysis of FRP anchorage zones with variable width. Compos Part B 2014; 67:410-426.

[158] Biscaia HC, Micaelo R, Teixeira J, Chastre C. Delamination process analysis of FRP-to-parent material bonded joints with and without anchorage systems using the Distinct Element Method. Compos Struct 2014; 116:104-119.

[159] Haddad H, Leclerc W, Guessasma M, Pélegris C, Ferguen N, Bellenger E. Application of DEM to predict the elastic behavior of particulate composite materials. Granul Matter 2015; 17:459-473.

[160] Ismail Y, Sheng Y, Yang D, Ye J. Discrete element modelling of unidirectional fibre-reinforced polymers under transverse tension. Compos Part B 2015; 73:118-125.

[161] Ismail Y, Yang D, Ye J. Discrete element method for generating random fibre distributions in micromechanical models of fibre reinforced composite laminates. Compos Part B

2016; 90:485-492.

[162] Maheo L, Dau F, André D, Charles JL, Iordanoff I. A promising way to model cracks in composite using Discrete Element Method. Compos Part B 2015; 71:193-202.

[163] Le BD, Dau F, Charles JL, Iordanoff I. Modeling damages and cracks growth in composite with a 3D discrete element method. Compos Part B 2016; 91:615-630.

[164] Che D, Saxena I, Han P, Guo P, Ehmann KF. Machining of carbon fiber reinforced plastics/polymers: A literature review. J Manufact Sci Eng 2014; 136:034001.

[165] Soussia AB, Mkaddem A, Mansori ME. Rigorous treatment of dry cutting of FRP – Interface consumption concept: A review. Int J Mech Sci 2014; 83:1-29.

[166] Iliescu D, Gehin D, Iordanoff I, Girot F, Gutiérrez ME. A discrete element method for the simulation of CFRP cutting. Compos Sci Technol 2010; 70:73-80.

[167] Ferguen N, Cogné C, Bellenger E, Guessasma M, Pélegris C. A numerical model for predicting effective thermal conductivities of alumina/Al composites. J Compos Mater 2013; 47:3311-3321.

[168] Pennec F, Alzina A, Tessier-Doyen N, Naït-ali B, Mati-Baouche N, De Baynast H, Smith DS. A combined finite-discrete element method for calculating the effective thermal conductivity of bio-aggregates based materials. Int J Heat Mass Transfer 2013; 60:274-283.

[169] Lu Z, Yuan Z, Liu Q, Hu Z, Xie F, Zhu M. Multi-scale simulation of the tensile properties of fiber-reinforced silica aerogel composites. Mater Sci Eng A 2015; 625:278-287.

[170] Shilko EV, Psakhie SG, Schmauder S, Popov VL, Astafurov SV, Smolin AY. Overcoming the limitations of distinct element method for multiscale modeling of materials with multimodal internal structure. Comput Mater Sci 2015; 102:267-285.

[171] Moreno-Atanasio R, Williams RA, Jia X. Combining X-ray microtomography with computer simulation for analysis of granular and porous materials. Particuology 2010; 81-99.

Figure captions

Fig. 1 Soft-body impact on a composite laminate. A CFRP cross-ply laminate, which was 165 mm long, 50 mm wide, and 1 mm thick, was fixed like a cantilever, and a gelatin ball with 20 mm diameter and 4.3 g mass was collided at the center of the plate at 155 m/s. The SPH model had fine spacing in the through-thickness direction, and the number of particles was 1040000 that was one fourth of the conventional SPH.

Fig. 2 Resin impregnation into fiber bundles. Particles representing air were initially arranged in and between bundles. Surface tension was taken into account between resin particles and fiber particles.

Fig. 3 Motion of hard balls in ball milling process. A nonlinear contact model based on the Hertzian stress was used for both steel balls and a circular steel wall. (a) Initial condition after free fall of balls. (b) Trajectory of all balls for 3 seconds under a constant rotating speed.

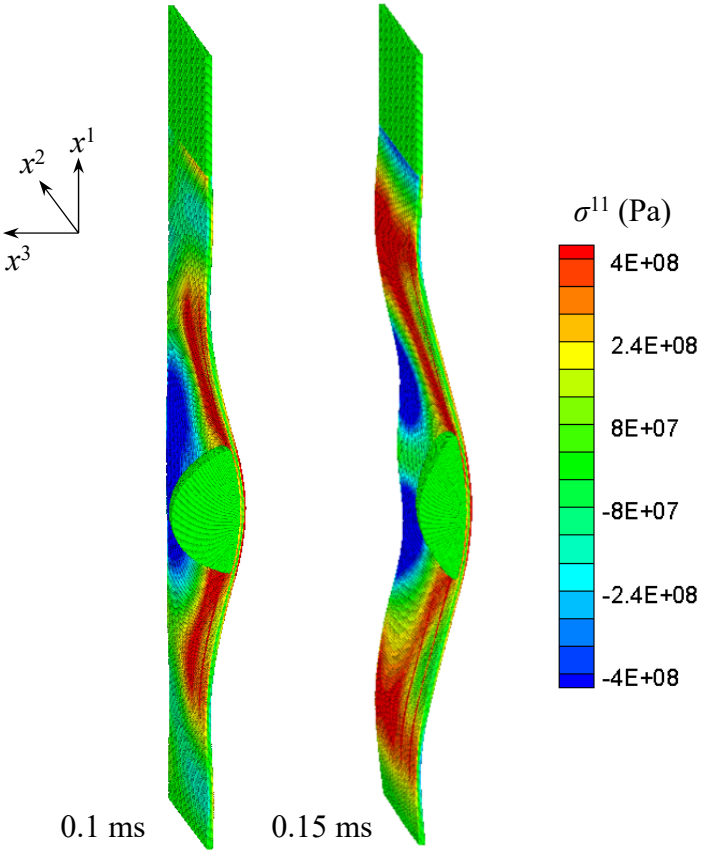

(a) Improved SPH simulation

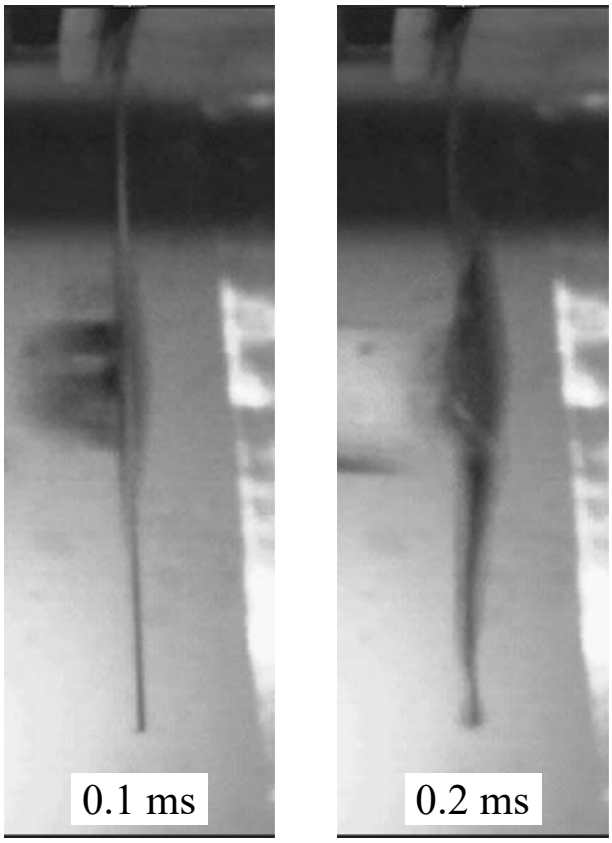

(b) High-speed camera image

Figure 1

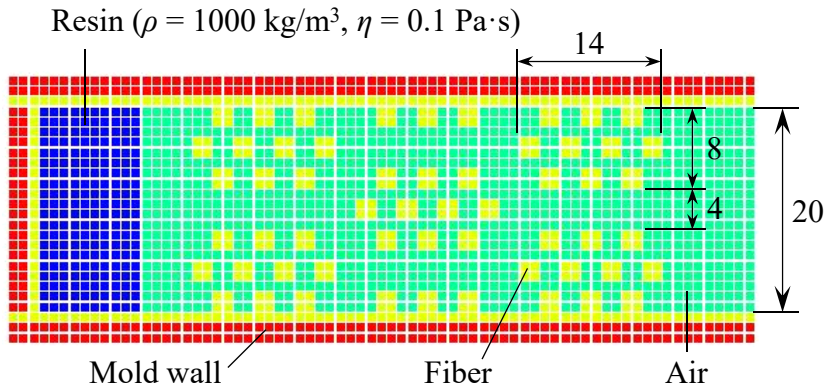

(a) Analytical model

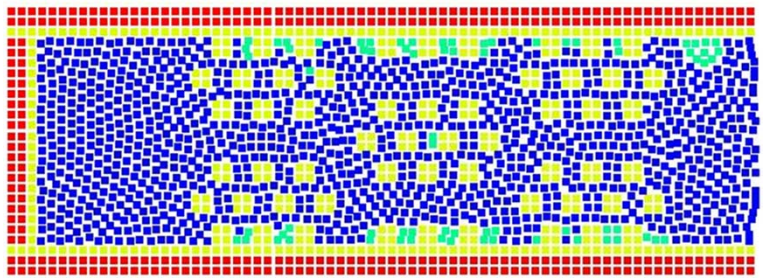

(b) High wettability (θ = 60º)

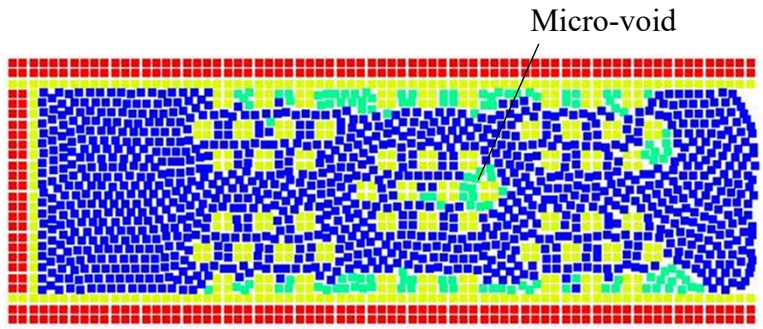

(c) Low wettability (θ = 120º)

Figure 2

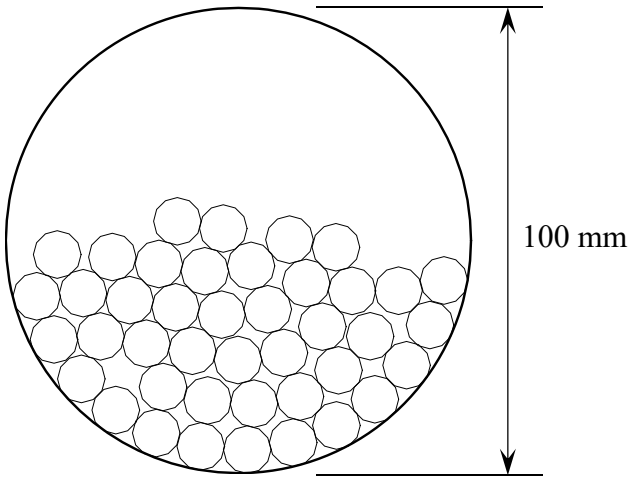

(a)

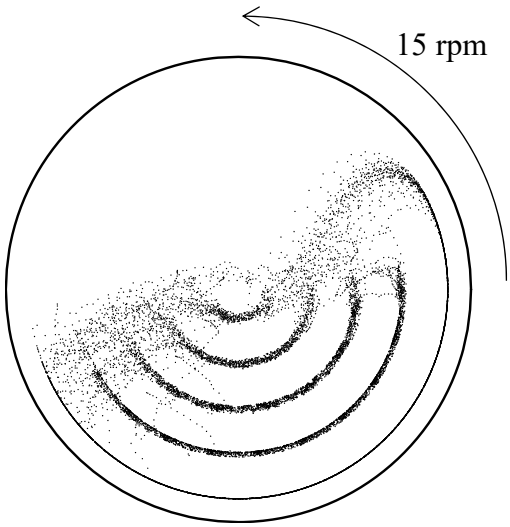

(b)

Figure 3